

Yüksek Sıcaklıkta Gaz Algılaması ve IR Kaynakları İçin Dayanıklı Microhotplate Dizaynı

Hasan GÖKTAŞ^{1*}

ÖZET: Microhotplate'ler (MHP) yüksek sıcaklıklarda gaz algılanması, ve IR kaynağı yapımı gibi çok önemli uygulama alanlarına sahip olmasına rağmen, göreceli yüksek sıcaklıklarda çalıştırıldıklarında oluşan yüksek termal stres'lerden dolayı kısa süreli dayanıklılığa sahiptirler. Bu çalışmada yüksek sıcaklıklarda düşük termal stres'e sahip bir dizaynı, spring tipi dizaynın ve termal genişleme sabitleri yakın olan malzeme seçiminin avantajlarını birleştirerek elde ettik. FEM sonuçları düşük termal stres elde edebilmesini sağlayan ana etkenin termal genişleme sabitleri yakın malzemeler seçmek olduğunu göstermiştir. SiN/Polysilicon/SiN katmanlarına ship spring tipi dizayn sayesinde 2119 K sıcaklığında 180 MPa gibi düşük termal stres FEM kullanılarak elde edilmiştir. Sıcaklığın 2076 K değerine ulaşması için gereken tepkime süresi ve güç tüketimi 200 ms ve 3.47 mW olarak hesaplanmıştır.

Anahtar kelimeler: Microhotplate, MEMS (mikroelektromekanik sistemler ve sensörler), düşük termal stres, yüksek sıcaklık, IR (infrared) kaynağı, gaz algılaması

Reliable Microhotplate Design for High temperature Gas Sensing and IR Source

ABSTRACT: While Microhotplates (MHPs) keeps very important place in many critical applications such as high temperature gas sensing and building IR source, they still suffer from short term reliability due to high thermal stress at relatively high temperatures. Here we demonstrate low thermal stress design at high temperatures by combining the advantages of spring type structure and compatible materials in terms of thermal expansion constant. FEM results demonstrated that, the main mechanism behind achieving low thermal stress is using compatible materials. A low thermal stress of 180 MPa at 2119 K was achieved by using SiN/Polysilicon/SiN stack with a spring type design via FEM tool. The response time required to reach 2076 K was calculated as 200 ms with 3.47mW power consumption.

Keywords: Microhotplate, MEMS (microelectromechanical systems and sensors), low thermal stress, ultra-high temperature, IR source, gas sensing

¹ Hasan GÖKTAŞ (Orcid ID: 0000-0002-2195-9531), Harran University, Electrical and Electronic Engineering, Şanlıurfa, Turkey

*Sorumlu Yazar / Corresponding Author: Hasan GÖKTAŞ, e-mail: hgoktas.gwu@gmail.com

INTRODUCTION

Microhotplate (MHP) has a wide range of applications that includes but not limited to gas sensors (Steinhauer et al., 2016; He et al., 2016), infrared sources (Barritault et al., 2011; Müller et al., 2014), a micro-chip initiator (Ahn et al., 2016), humidity sensors (Sama et al., 2017), and thermo-optical characterization (Chauhan et al., 2014), nanowire and carbon nanotube growth (Sama et al., 2017; Silvestri et al., 2016) and characterization (Silvestri et al., 2016). Miniaturized gas sensors, among those other applications, is getting more attraction especially in internet of things (IOT) applications. Most well-known examples are food quality monitoring (Peris and Escuder-Gilabert, 2009), automotive industry (Yamazoe, 2005) and agriculture (Mitzner et al., 2003). Many different techniques and solutions have been offered to address the temperature uniformity with different heater structures (Graf et al., 2006; Roy et al., 2012), high temperature operation with reliability (Barritault et al., 2011; Richter and Fritze, 2013; Govindhan et al., 2018), and smaller response time (Mo et al., 2002; Huang et al., 2009). MHP with high temperature operation (up to 1000 °C) is very demanding in the gas sensor field. It brings the possibility to monitor especially combustion gas components such as HCs, CO and NO_x and consequently allows emission control (Liu et al., 2014; Govindhan et al., 2018). Furthermore, fast thermal response for gas sensing can be achieved at high temperature (900 °C) (Richter and Fritze, 2013) and this enables not only real-time characterization of nanomaterials (Mele et al., 2012) but also temperature modulation for selective gas sensing (He et al., 2016). In the same way, hydrogen gas sensors operate above 500 °C (Govindhan et al., 2018), oxygen sensors up to 1400 °C (Chowdhury et al., 2001), Ga₂O₃ layer for reducing gases and O₂ detection between 600 and 900 °C (Schwebel et al., 2000) and CeO₂ layer for Co and N₂ detection between 800 and 1000 °C (Liu et al., 2014). In

addition to gas sensors, building IR source also requires high temperature capable MHP and this brings the necessity of reliability (mechanical, electrical, etc..) at high temperatures. MHP based IR sources was demonstrated (Barritault et al., 2011) with an operating temperature of 650 °C and in (Müller et al., 2014) with an operating temperature around 700 °C.

Materials with different thermal expansion constants results in high thermal stress at relatively high temperature and this consequently cause device failure. Although high temperature is achieved in (Mele et al., 2012) by using special material (Molybdenum), it could only work approximately 24 hours before breakage. However; long-term stability is very important especially for the high temperature MHP gas sensors and IR sources and this requires very low thermal stresses design.

Here we designed an MHP with low thermal stress in a well-known silicon process by using FEM tool. The multilayer approach was used to ensure the electrical isolation and a robust platform that allows a deposition process for sensing layer. Three different designs were used and compared, while design 1 and design 2 show the advantages of using spring type structure over conventional type design, design 1 and design 3 show the advantages of selecting optimum materials for the sake of low thermal stress. The thermal stress was decreased from 2000 MPa to 180 MPa by selecting materials' thermal expansion constants as close as possible to each other. A uniform temperature distribution with a total of 5 K (0.2%) difference on MHP's surface was achieved via optimizing heater and bridge design with spring type design. Furthermore, the response time and power consumption to reach 2076 K was found as 200 ms and 3.47 mW respectively via FEM tool while limiting the maximum thermal stress to 180 MPa for optimum design.

MATERIALS AND METHODS

Basic MHP design consists of two dielectric layers (layer 1 & 3) for electrical isolation and one conductor layer (layer 2) as a heater. Two different structures and two different fabrications were studied throughout the paper. Design 1 is a

spring type MHP (Fig 1A) where layer 1 & 3 are silicon nitride (SiN) and layer 2 is Polysilicon. Design 2 is a conventional type MHP (Fig 1B) whereas design 3 is a spring type MHP (Fig 1A) where layer 1 & 3 are silicon dioxide (SiO₂) and layer 2 is Polysilicon for both design 2 & 3.

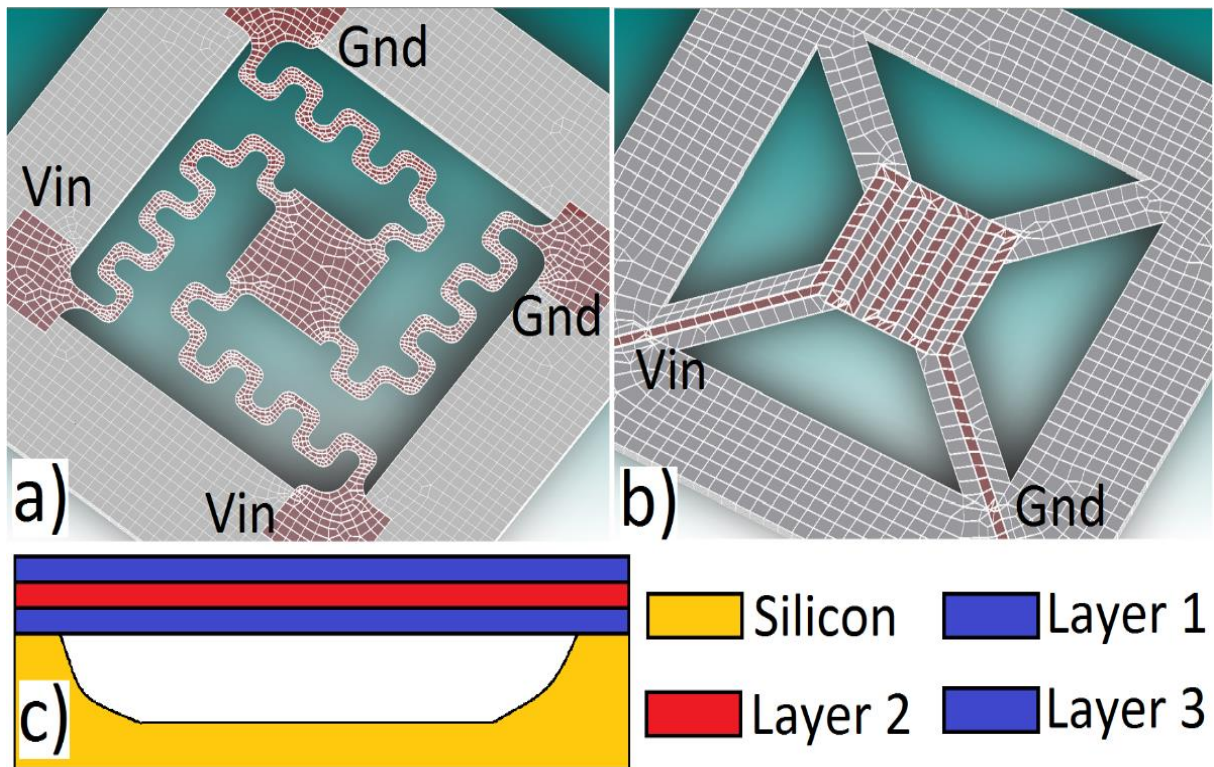


Figure 1. (A) Spring type MHP, (B) Conventional type MHP, (C) Cross Section View of MHP

It is well known from CMOS process that SiO₂ and Polysilicon can be deposited and patterned on top of each other as they have fabrication compatibility and good etch selectivity. In the same way, both SiN and Polysilicon can be deposited in the same fabrication process and this fabrication compatibility was verified in (Yu et al., 1996). The fabrication starts with deposition of layer 1. After step 1, heater (layer 2) was deposited on layer 1 and patterned with a mask in lithography process and dry etch process. After patterning layer 2, the layer 3 was deposited on layer 2. The final step is to use XeF₂ etch process to release the MHP structure by removing silicon layer underneath the layer 1.

RESULTS AND DISCUSSION

Uniform heating

The operation principle of MHP design is based on applying voltage on heater element to create joule heating that results in non-uniform temperature distribution. Heater structure in spring type MHP (Fig 1A) consists of four legs where two of them are Vin and two of them are ground. On the other hand, heater in conventional type MHP (Fig 1B) consists of two legs with a serpentine structure. One of the main problem with serpentine structure is the non-uniform joule heating profile. That's why the center plate in spring type MHP was designed as a single part to enable uniform temperature distribution (Fig 1A). The maximum temperature in both spring and

conventional design (Fig 2) was set above 2000 K via joule heating. A very uniform temperature profile with a 5 K (2120-2115) difference throughout the MHP plate in spring type design was achieved and verified via FEM simulation (Fig 2B). On the other hand, the temperature difference is 223 K (2043-1820) throughout the MHP plate in conventional type design according

to FEM simulation (Fig 2A). The temperature difference in spring type structure can be less than 0.2%, while it is approximately 11% in conventional serpentine design. In another words, a 55x times improvement can be achieved via spring type heater in comparison to serpentine type heater.

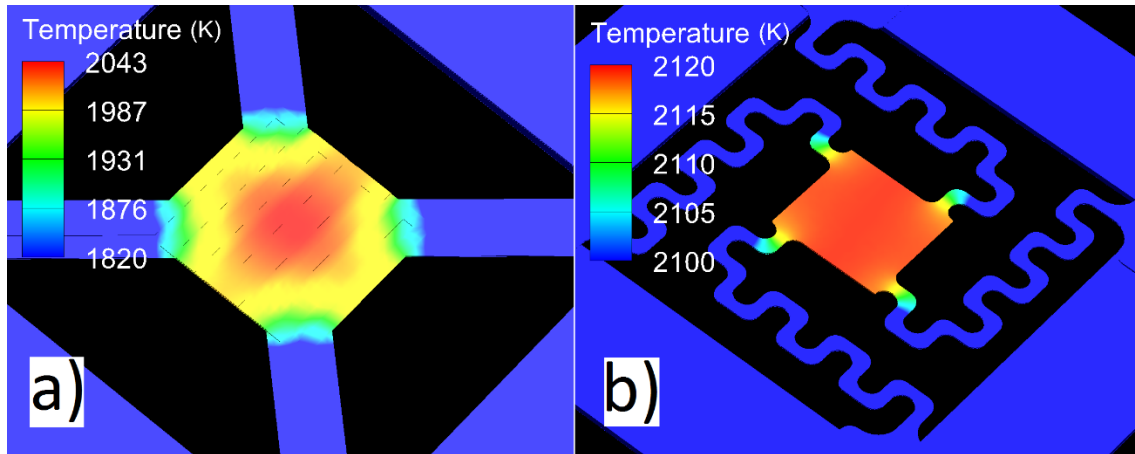


Figure 2. Temperature distribution on (A) Conventional type design, and (B) Spring type design via FEM

Low thermal stress design

Difference in thermal expansion constants between layers is the most well-known and common reason for the thermal stress at relatively high temperatures. This especially creates

$$\sigma_{xi}(y) = -\alpha E_i T_i(y) + E_i \frac{P_T I_{E2} - M_T I_{E1}}{I_{E0} I_{E2} - I_{E1}^2} + y E_i \frac{M_T I_{E0} - P_T I_{E1}}{I_{E0} I_{E2} - I_{E1}^2} \quad (1), \text{ where;}$$

$$I_{EX} = \frac{1}{X+1} \sum_{i=1}^n E_i w_i (y_i^{X+1} - y_{i-1}^{X+1}), \quad P_T = \sum_{i=1}^n \int_{y_{i-1}}^{y_i} \alpha_i E_i T_i(y) w_i dy, \quad M_T = P_T y$$

Here T is the temperature, E is the elastic modulus, y is the thickness, and α is the thermal expansion constant. The thermal stress will increase with the increase in the number of layers according to equation 1 and it will get worse if the difference in thermal expansion constant of materials is larger. This can be explained by the increase in M_T , P_T and the first term in equation 1.

Three different designs (design 1, 2 & 3) were tested in FEM simulation to study the effect of thermal stresses with respect to temperature (Fig 3). The thermal expansion of Polysilicon is

problems with multilayer processes such as CMOS, that is widely used in building sensors, and microprocessor. The thermal stress for composite structure (Noda et al., 2003) is;

$2.32 \times 10^{-6} K^{-1}$ while it is $0.5 \times 10^{-6} K^{-1}$ for SiO_2 and $1.6 \times 10^{-6} K^{-1}$ for SiN . Here Polysilicon is a conductive heater layer while SiO_2 and SiN were used as a dielectric layer and supportive layer for the MPH bridges.

The maximum thermal stress was 2000 MPa (Fig 3C) at 1942 K due to large difference in thermal expansion constants of SiO_2 and Polysilicon. This high thermal stress was decreased to 550 MPa at 2043 K by replacing SiO_2 with SiN in conventional type design (Fig 3B). This is attributed to the fact that, the difference in thermal expansion constant between SiN and Polysilicon

$(2.32 \times 10^{-6} - 1.6 \times 10^{-6} = 0.72 \times 10^{-6})$ is smaller than the one between SiO_2 and Polysilicon $(2.32 \times 10^{-6} - 0.5 \times 10^{-6} = 1.82 \times 10^{-6})$. However, 550 MPa is still too high and can easily result in failure. More improvement was achieved via using spring structure design with Polysilicon as a heater layer and SiN as a dielectric layer (Fig 3A). As a result, the maximum thermal stress was decreased from 550 MPa to 180 MPa at 2119 K. Here spring structure, in contrast to conventional type design (Fig 3B), allows more thermal expansion and consequently helps in decreasing the overall thermal stress. The thermal stress with respect to temperature is reasonably small even at high temperatures for design 1, on the other hand thermal stress drastically increases with the increase in the temperature for design 2 & 3 (Fig 3D). This

makes design 1 a perfect candidate for high temperature gas sensing and building an IR source with a long-term stable operation. The ultimate/tensile strength for SiN is 390 MPa (Cardinale and Tustison, 1992), for SiO_2 is 200 MPa (Morozov and Postnikov, 2014) and for Polysilicon is 1200 MPa (Sharpe et al., 1997) and all are well above the thermal stresses of 120 MPa at 1374 K and 180 MPa at 2119 K for design 1. This low thermal stress provides a safety factor (safety factor = ultimate stress / actual stress) of 3.25 $(390/120)$ at 1374 K and 2.2 $(390/180)$ at 2119 K. On the other hand, design 3 and design 2 fails at even low temperature because both designs already exceed the limit of 200 MPa tensile strength of SiO_2 and 390 MPa tensile strength of SiN.

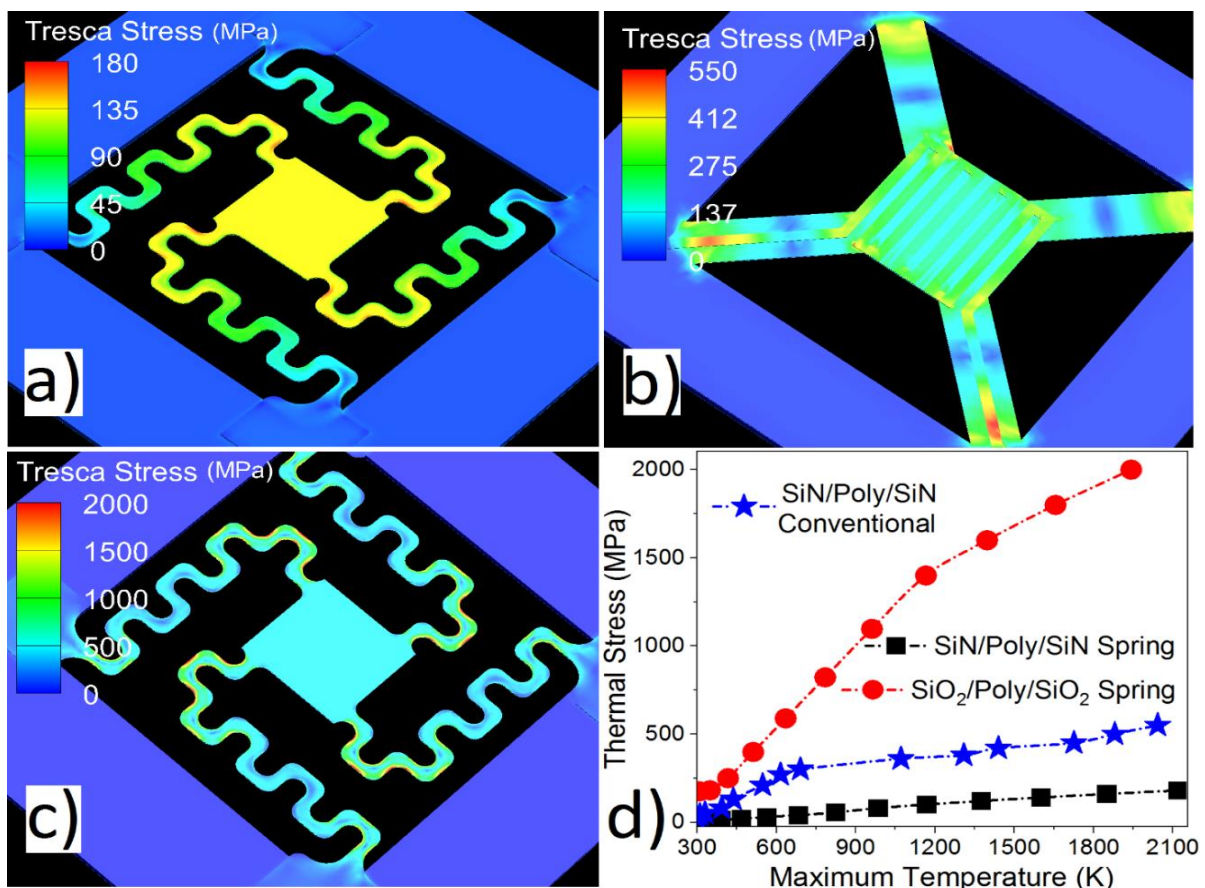


Figure 3. Thermal stress above 2000 K for (A) SiN/Polysilicon/SiN Spring type design (design 1), (B) SiN/Polysilicon/SiN Conventional type design (design 2), (C) SiO₂/Polysilicon/SiO₂ Spring type design (design 3), and (D) Thermal stress comparison between three different designs via FEM simulation

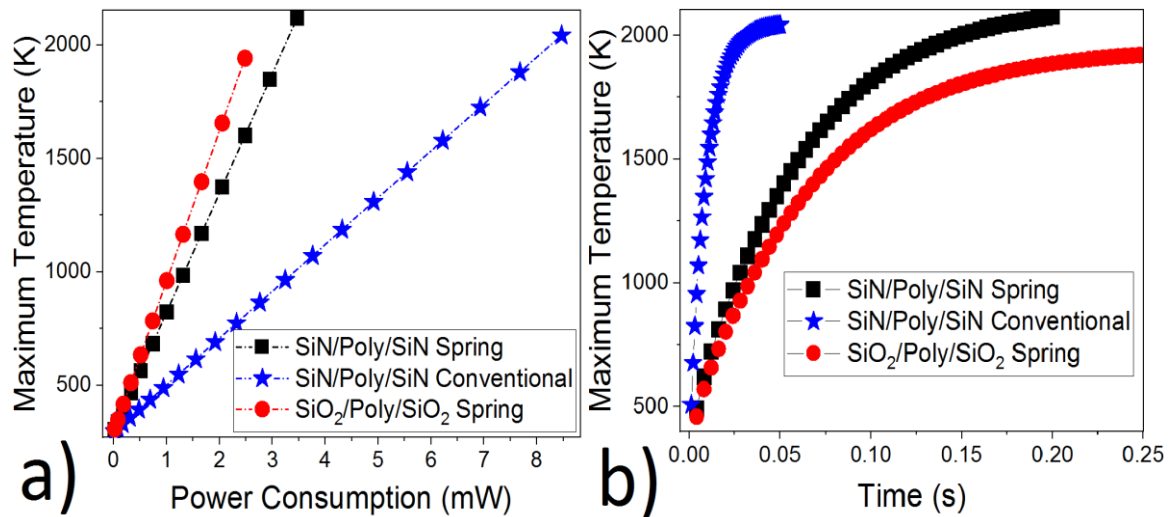


Figure 4. The performance comparison between Design 1, 2 & 3 via FEM simulation in terms of (A) Transient time response and (B) Power consumption to reach 2000 K

Response time and power consumption

The temperature profile and the maximum temperature with respect to applied bias voltage can be found via thermal conduction equation;

$$\Delta T = \frac{q' L^2}{2k} \quad (2)$$

Where ΔT is the temperature difference throughout the MHP bridges, q' is the heat generation, L is the bridge length and k is the thermal conduction constant.

Conventional design (design 2) has shorter and wider bridges compared to spring type design (design 1) that results in more heat loss throughout the beams and consequently smaller ΔT . This brings the necessity to apply higher power for the same amount of heat generation. Hence, it takes around 8.47 mW power consumption to reach 2043 K for design 2 while the power consumption for design 1 is 3.47 mW to reach 2119 K. In addition, design 3 takes less power (2.48 mW) to reach 1942 K in comparison to design 1 due to smaller thermal conductivity constant ($k_{\text{SiO}_2} (1.4 \times 10^6) < k_{\text{SiN}} (3.2 \times 10^6)$) (Fig 4A).

The transient time response is dominated by the power required to reach above 2000 K according to FEM simulation and this is attributed to the fact that, ΔT is proportional to the heat

generation (equation 2). It takes 50 ms and 8.47 mW for design 2, 200 ms and 3.47 mW for design 1 and 248 ms and 2.48 mW for design 3 (Fig 4B) to reach above 2000 K.

CONCLUSION

High thermal stress is one the most challenging design issue for the MHP and prevents its long-term usage in high temperature gas sensing and building a high temperature IR source. Here we presented solution methods to address the high thermal stress problem. Tough spring type design allows more thermal expansion compared to conventional design; it still results in high thermal stress that is not acceptable for long term reliable MHP design. On the other hand, using compatible materials drastically decreased the thermal stress even for conventional type design. An ultra-low thermal stress of 180 MPa at 2119 K was achieved by combining spring type design with compatible material stack in terms of thermal expansion constant (SiN/Polysilicon/SiN stack). The design promises a 3.47 mW power consumption with a 200 ms to reach 2076 K. These results open a way to design high temperature gas sensors (>1000 °C) for critical applications (sensing combustion gases, etc) and IOT applications in addition to building long term reliable IR sources.

REFERENCES

- Ahn JY, Kim SB, Kim JH, Jang NS, Kim DH, Lee HW, Kim JM, and Kim SH, 2016. A microchip initiator with controlled combustion reactivity realized by integrating Al/CuO nanothermite composites on a microhotplate platform. *IOP Journal of Micromechanics and Microengineering*, 26(1):1-10
- Barritault P, Brun M, Gidon S, Nicoletti S, 2011. Mid-IR source based on a free-standing microhotplate for autonomous CO₂ sensing in indoor applications. *Elsevier Sensors and Actuators A: Physical*, 172: 379-385
- Cardinale GF, Tustison RW, 1992. Fracture strength and biaxial modulus measurement of plasma silicon nitride films. *Elsevier Thin Solid Films*, 207: 126-130
- Chauhan VM, Hopper RH, Ali SZ, King EM, Udrea F, Oxley CH, Aylott JW, 2014. Thermo-optical characterization of fluorescent rhodamine B based temperature-sensitive nanosensors using a CMOS MEMS micro-hotplate. *Elsevier Sensors and Actuators B: Chemical*, 192: 126-133
- Chowdhury AKMS, Akbar SA, Kapileshwar S, Schorr JR, 2001. A rugged oxygen gas sensor with solid reference for high temperature applications. *Journal of the electrochemical society*, 148: G91-G94
- Graf M, Barrettino D, Kirstein KU, Hierlemann A, 2006. CMOS microhotplate sensor system for operating temperatures up to 500. *Elsevier Sensors and Actuators B: Chemical*, 117: 346-352
- Govindhan M, Sidhureddy B, Chen A, 2018. High Temperature Hydrogen Gas Sensor Based on Three-Dimensional Hierarchical Nanostructured Nickel-Cobalt Oxide. *ACS Applied Nano Materials*, 1: 6005-6014
- He A, Yu J, Wei G, Chen Y, Wu H, Tang Z, 2016. Short-Time Fourier Transform and Decision Tree-Based Pattern Recognition for Gas Identification Using Temperature Modulated Microhotplate Gas Sensors. *Journal of Sensors*, 2016: 1-12.
- Huang WC, Chen CN, Shen SH, Chen CC, 2009. Study of the annealing effect of low-temperature oxide on the etch rate in TMAH solutions for microheater applications. 2009 IEEE 3rd International Conference on Nano/Molecular Medicine and Engineering, 18-21 October 2009, Tainan, Taiwan
- Liu Y, Parisi J, Sun X, Lei Y, 2014. Solid-State Gas Sensors for High Temperature Application – A review. *RCS Journal of Material Chemistry A*, 2: 9919-9943
- Mitzner KD, Sternhagen J, Galipeau DW, 2003. Development of a micromachined hazardous gas sensor array. *Elsevier Sensors and Actuators B: Chemical*, 93: 92-99
- Mele L, Santagata F, Iervolino E, Mihailovic M, Rossi T, Tran AT, Schellevis H, Creemer JF, Sarro PM, 2012. A molybdenum MEMS microhotplate for high-temperature operation. *Elsevier Sensors and Actuators A: Physical*, 188: 173-180
- Mo Y, Okawa Y, Inoue K, Natukawa K, 2002. Low voltage and low-power optimization of micro-heater and its on-chip drive circuitry for gas array. *Sensors and Actuators A: Physical*, 100: 94-101
- Morozov O, Postnikov A, 2014. Mechanical strength study of SiO₂ isolation blocks merged in silicon substrate. *IOP Journal of Micromechanics and Microengineering*, 25: 1-11

- Müller L, Kapplinger I, Biermann S, Brode W, Hoffmann M, 2014. Infrared emitting nanostructures for highly efficient microhotplates” IOP Journal of Micromechanics and Microengineering. 24: 1-9
- Noda N, Hetnarski RB, Tanigawa Y, 2003. Thermal Stresses, Second Edition, New York, USA, 493 p.
- Peris M, Escuder-Gilabert L, 2009. A 21st century technique for food control: Electronic noses. *Analytica Chimica Acta*, 638: 1-15
- Richter D, Fritze H, 2013. High temperature Gas Sensor. Springer Series on Chemical Sensors and Biosensors, 1-46p.
- Roy S, Sarkar CK, Bhattacharyya P, 2012. A highly sensitive methane sensor with nickel alloy microheater on micromachined Si substrate. Elsevier Solid-State Electronics, 76: 84-90
- Sama J, Seifner MS, Domenech-Gil G, Santander J, Calaza C, Moreno M, Gracia I, Barth S, Romano-Rodriguez A, 2017. Low temperature humidity sensor based on Ge nanowires selectively grown on suspended microhotplates. Elsevier Sensors and Actuators B: Chemical, 243: 669-677
- Schwebel T, Fleischer M, Meixner H, 2000. A selective, temperature compensated O₂ sensor based on Ga₂O₃ thin films. Elsevier Sensors and Actuators B: Chemical, 65: 176-180
- Sharpe WN, Yuan JB, Vaidyanathan R, 1997. Measurements of Young's modulus poisson's ratio, and tensile strength of polysilicon. Proceedings IEEE The Tenth Annual International Workshop on Micro Electro Mechanical Systems. An Investigation of Micro Structures, Sensors, Actuators, Machines and Robots, 26-30 January 1997, Nagoya, Japan
- Silvestri C, Riccio M, Poelma RH, Morana B, Vollebregt S, Santagata F, Irace A, Zhang GQ and Sarro PM, 2016. Thermal characterization of carbon nanotube foam using MEMS microhotplates and thermographic analysis. *RCS Nanoscale*, 15:1-10
- Steinhauer S, Chapelle A, Menini P, Sowwan M, 2016. Local CuO Nanowire Growth on Microhotplates: In Situ Electrical Measurements and Gas Sensing Application. *ACS Sensors*, 1: 503-507.
- Yamazoe N, 2005. Toward innovations of gas sensor technology. Elsevier Sensors and Actuators B: Chemical, 108: 2-14
- Yu S, Gulari E, Kanicki J, 1996. Selective deposition of polycrystalline silicon thin films at low temperature by hot wire chemical vapor deposition. *Applied Physics Letters*, 68: 2681-2683